9-2018

The contribution of local and transport processes to phytoplankton biomass variability over different timescales in the Upper James River, Virginia

Qubin Quin
Virginia Institute of Marine Science

Jian Shen
Virginia Institute of Marine Science

Recommended Citation

Quin, Qubin and Shen, Jian, The contribution of local and transport processes to phytoplankton biomass variability over different timescales in the Upper James River, Virginia (2018). *Estuarine, Coastal and Shelf Science*, 196, 123-133.
https://doi.org/10.1016/j.ecss.2017.06.037

The contribution of local and transport processes to phytoplankton biomass variability over different timescales in the Upper James River, Virginia

Qubin Qin* and Jian Shen

Virginia Institute of Marine Science, College of William and Mary,

Gloucester Point, VA, 23062, USA

*Corresponding Author:

Qubin Qin

Virginia Institute of Marine Science

College of William and Mary

Gloucester Point, VA 23062

Email: qubin@vims.edu

Phone: (804) 684-7670

The contribution of local and transport processes to phytoplankton biomass variability over different timescales in the Upper James River, Virginia

Qubin Qin* and Jian Shen

Virginia Institute of Marine Science, College of William and Mary,

Gloucester Point, VA, 23062, USA

Abstract

Although both local processes (photosynthesis, respiration, grazing, and settling), and transport processes (advective transport and diffusive transport) significantly affect local phytoplankton dynamics, it is difficult to separate their contributions and to investigate the relative importance of each process to the local variability of phytoplankton biomass over different timescales. A method of using the transport rate is introduced to quantify the contribution of transport processes. By combining the time-varying transport rate and high-frequency observed *chlorophyll a* data, we can explicitly examine the impact of local and transport processes on phytoplankton biomass over a range of timescales from hourly to annually. For the Upper James River, results show that the relative importance of local and transport processes differs on different timescales. Local processes dominate phytoplankton variability on daily to weekly timescales, whereas the contribution of transport processes increases on seasonal to annual timescales and reaches equilibrium with local processes. With the use of the transport rate and high-frequency *chlorophyll a* data, a

method similar to the open water oxygen method for metabolism is also presented to estimate phytoplankton primary production.

Keywords: Transport rate; phytoplankton biomass; high-frequency observational data; primary production; timescale; open water method

1. Introduction

Phytoplankton dynamics, such as the variability of biomass at a location, are controlled by both local processes and physical transport processes. Local environmental conditions, such as temperature, light, nutrient supply, and grazing pressure, strongly regulate phytoplankton growth and primary production through both bottom-up and top-down controls (Kremer and Nixon, 1978). Transport processes in aquatic systems, including advective transport and diffusive transport, affect phytoplankton biomass by redistributing either biomass (direct effect), or dissolved and particulate constituents such as nutrients that regulate phytoplankton growth (Lucas et al., 1999; Cloern, 2001; Paerl et al., 2006; Lancelot and Muylaert, 2011).

The interactions between local and transport processes are complex, and their contributions to phytoplankton dynamics can vary under different dynamic conditions. Because each external forcing (e.g. tide, flow, and wind) and environmental factor (light and temperature) has its own periodic fluctuation, the fluctuation will affect these two processes. We hypothesize that the relative importance of local and transport processes varies with timescales, which is also indicated by previous literature. Lucas et al. (2006) suggest that intra-daily variability of phytoplankton biomass is largely controlled by both the diurnal light cycle and the semidiurnal tidal oscillation, which implies the importance of contributions from both local environmental conditions and tide on the hourly timescale. Lake et al (2013) conduct measurements of photosynthetic rates and integrate daily production on summer months in the York River for both the spring and neap tides. They find that daily primary production does not show a clear variation

during spring-neap cycle, which suggests that the local biological processes are dominant for daily primary production rather than transport processes. Shen et al. (2008) show that the high biomasses of macroalgae and phytoplankton are the dominant cause of diurnal variation of dissolved oxygen concentration (DO) resulting from high production during daytime and high respiration at night. It suggests that local biological processes can be the dominant processes for primary production for the daily timescale in estuaries and shallow-water systems. Conversely, changes in freshwater discharge are considered to be a major factor driving strong seasonal and annual patterns of phytoplankton biomass in river-dominated estuaries, which modulate the location and strength of algal blooms through transport and nutrient supply (Valdes-Weaver et al., 2006; Reaugh et al., 2007; Costa et al., 2009; Peierls et al., 2012). Bukaveckas et al. (2011) show that algal blooms vary longitudinally along the Upper James River, and peak at the location where residence time becomes large due to a change of geometry, where about two-thirds of the net primary production is respired locally, and the remaining one-third is transported out of the region by fluvial and tidal advection. It suggests that the variability of phytoplankton biomass can be altered by a dynamic condition resulting from a change of local geometry.

These studies point out the relative importance of transport processes compared to local biological processes on particular timescales. However, due to the difficulty to explicitly separate their contributions, few contributions to the literature discuss how the comparison changes over a range of timescales from days to years though which is interesting to know for some studies. For example, Lucas et al. (2009) suggest that the

variability of phytoplankton biomass can be described by a steady-state balance between local biological processes and transport processes described by residence time (i.e., it assumes that the variability of phytoplankton biomass is negligible, and local and transport processes are equal but counterbalanced in contribution). While this steady-state balance assumption may hold for long-term timescales, it is questionable for short-term timescales, such as daily and weekly timescales. A relevant discussion on the comparison of relative importance of the two processes is helpful to answer on what range of timescales the assumption is valid.

The relative importance of each process on phytoplankton dynamics also needs to be evaluated for studies based on *in situ* observational data. As the development of instruments, many water quality parameters like DO and *chlorophyll-a* fluorescence can be measured *in situ* at 15-minute intervals, which is often referred to as high-frequency data (http://web2.vims.edu/vecos/). The easy accessibility of high-frequency DO data has prompted wide applications of the open water method for estimating ecosystem primary production and metabolism (Odum, 1956; Howarth and Michaels, 2000; Cole et al., 2000; Caffrey, 2004; Kemp and Testa, 2011). When applying this method for estimating daily ecosystem primary production and metabolism, the effect of physical transport processes is usually neglected (Staehr et al., 2010). This estimation without considering transport, however, may have large biases when biological metabolism or DO is significantly influenced by transport processes (Kemp and Boynton, 1980). In the discussion section of this study, we applied a similar open water method to estimate phytoplankton primary production using high-frequency *chl-a* concentration (denoted

by *chl-a*) data. The question as to whether the approach will cause more bias using phytoplankton data is unknown as spatial horizontal gradients of *chl-a* are often larger than those of DO. To evaluate the approach, the contribution of the transport processes on the daily timescale needs to be addressed.

The objective of this study is to evaluate how the relative importance of local and transport processes to the local variability of phytoplankton biomass vary over a range of timescales from hours to years. Because the transport processes not only affect the phytoplankton biomass but also affect the nutrient transport, when evaluating the relative importance of transport processes to biomass variability, the contribution of transport processes is restricted to the direct effect that redistributes biomass, and therefore other indirect effects that regulate phytoplankton growth, such as temperature, light availability, and nutrient limitation, are attributed to the contribution of local processes. The Upper James River was selected as the study site where both local and transport processes contribute greatly to phytoplankton dynamics (Bukaveckas et al., 2011).

2. Methods

In this section we first presented how to attribute the variability of phytoplankton biomass to the contributions of local and transport processes separately by decomposing the transport equation. Then we presented a detailed procedure to compute each contribution by using *in situ* observational phytoplankton data and dynamic fields. The phytoplankton biomass dynamics and contribution of local

processes were estimated using observational data, while the contribution of transport processes was estiamted using dynamic fields computed by a dynamic model. Lastly, we statistically analyzed to evaluate the relative importance of local and transport processes, repectively, over a range of timescales.

2.1. Decompose change of biomass

The observation of phytoplankton data can be described by a three-dimensional transport equation with source and sink terms (Chapra, 1997). For simplicity, the first-order reaction transport equation for volumetric phytoplankton biomass in the *x*-direction can be expressed as follows:

$$\frac{\partial C}{\partial t} + u\frac{\partial C}{\partial x} - \frac{\partial}{\partial x}\left(K\frac{\partial C}{\partial x}\right) = gC \quad (1)$$

where *C* denotes volumetric phytoplankton biomass (g C m^{-3}), *x* and *t* denote location and time, respectively, *u* is current velocity (m s^{-1}), *K* is diffusivity (m^2 s^{-1}), and *g* denotes the growth rate of phytoplankton (d^{-1}) as a result of local processes. We combined growth and loss as a net growth term *g*, as $g = G - R - M$, where *G* is the gross growth rate, *R* is the respiration/excretion rate, and *M* is the mortality rate due to both grazing and settling. The gross growth rate *G* is a function of available light, nutrients, and temperature (Chapra, 1997). Note that Eq. (1) only includes terms in the *x*-direction for making the following derivations clear and all variables vary vertically. The terms on the left-hand side of Eq. (1) are the time derivative term, advective transport, and diffusive transport, respectively. Transport processes may increase local concentration of a property if the incoming water has higher concentrations, or decrease it if the

incoming water has lower concentrations. Thus, the impact of transport processes does not only depend on hydrodynamic fields (*u* and *K*) but also on the horizontal gradient of phytoplankton biomass ($\partial C/\partial x$).

Areal phytoplankton biomass (g C m^{-2}) can be conventionally obtained by vertical integration of volumetric phytoplankton biomass *C* from the bottom to the surface, i.e., $B = \int_0^H Cdz$, where *z* is the vertical location, and *H* is the water depth (m), $B = C \cdot H$ if the water column is well-mixed. As no phytoplankton is transported across the surface or the bottom, integrating Eq. (1) gives the transport equation for areal phytoplankton biomass:

$$\frac{\partial B}{\partial t} + \int_0^H \left[u\frac{\partial C}{\partial x} - \frac{\partial}{\partial x}\left(K\frac{\partial C}{\partial x}\right)\right] dz = g_B B \quad (2)$$

where g_B is the vertical mean growth rate that accounts for the growth of areal biomass *B*.

Analogous to the algal growth for biological process, we express transport processes as a transport rate F_B, which is defined as

$$F_B = \frac{1}{B}\int_0^H \left[u\frac{\partial C}{\partial x} - \frac{\partial}{\partial x}\left(K\frac{\partial C}{\partial x}\right)\right] dz, \quad (3)$$

and the governing equation (1) can be transformed into the expression:

$$\frac{\partial B}{\partial t} = (g_B - F_B)B \quad (4)$$

Dividing Eq. (4) by *B* on both sides gives the equation for the rates:

$$\frac{1}{B}\frac{\partial B}{\partial t} = g_B + (-F_B) \quad (5)$$

Note that the impact of transport processes, expressed by F_B in Eq. (3), depends on $\partial C/\partial x$. The non-zero $\partial C/\partial x$ can be caused by either the change of dynamic conditions due to interaction between forcings (i.e., flow, tide) and geometry, or the spatially inhomogeneous local biological processes. Thus, the contribution of transport processes in fact comes from both the dynamically induced transport (referred to as physical transport) and the non-physical transport. The contribution of non-physical transport can be expected to be relatively small locally as biological processes have less spatial gradient compared to the physical transport. Our interest is to understand the physical transport that contributes the change of biomass. We introduce transport rate *F* that only expresses the physical transport and we can now write Eq. (5) as follows:

$$\begin{aligned} r &= \underbrace{g_B}_{Local} + \underbrace{(-F)}_{Physical\ Transport} + \underbrace{(F - F_B)}_{Non-physical\ transport} \\ &= \underbrace{\mu}_{Local^*} + \underbrace{(-F)}_{Physical\ Transport} \end{aligned} \quad (6)$$

where r is the rate to express the variability of phytoplankton biomass as $r = \frac{1}{B}\frac{\partial B}{\partial t} = \frac{\partial lnB}{\partial t}$, and can be estimated from *in situ* observations of phytoplankton biomass *B*. The physical transport rate F is unknown but it can be estimated by using hydrodynamic field and boundary conditions. $\mu = g_B + (F - F_B)$, which represents the growth rate of biomass that resulted from the combined local contributions. Once we know both values of *r* and *F*, μ can be computed as (*r* – *F*). When g_B is zero (such as conservative properties) or it is spatially homogenous, F equals F_B, and μ equals g_B. We will refer to *r* as the relative growth rate, and to μ as the effective growth rate in the following sections. As *F* only represents the transport contribution, a negative *F* value corresponds

178 to a “transport in” process that increases biomass, and a positive *F* value corresponds to
179 a “transport out” process that decreases biomass in accordance with Eq. (6), and a zero
180 *F* means there is no contribution of transport processes on local phytoplankton
181 variability.

182 Eq. (6) demonstrates that the relative change of biomass is a result of competition
183 between local and transport processes, and their contributions could be evaluated by
184 comparing the effective growth rate μ to the transport rate F:

185 1) $\mu > F$ leads to $r > 0$, biomass increases
186 2) $\mu < F$ leads to $r < 0$, biomass decreases
187 3) $\mu = F$ leads to $r = 0$, biomass remains constant

188 Note that μ and F could both have negative values. For example, the observed biomass
189 *B* at a location may increase at night ($r > 0$) when photosynthesis does not occur ($\mu < 0$),
190 but biomass can increase due to a transport of biomass to this location ($F < 0$,
191 “transport in”).

192 *2.2. Study site*

193 The James River is a tributary of the lower Chesapeake Bay located along the U.S. East
194 Coast (Fig. 1). The Upper James River is the tidal freshwater region where salinity is
195 between 0 and 0.05. Calibrated time series data (15-minute intervals) were collected
196 from Chesapeake Bay Continuous Monitoring Station JMS073.37 at the Virginia
197 Commonwealth University Rice Rivers Center (‘RC’, green triangle,
198 http://web2.vims.edu/vecos/), from March to November 2006, 2007, and 2008. Data

199 were measured using YSI 6600 data sondes with the Clean Sweep Extended Deployment
200 System, include a number of parameters such as *chl-a*, temperature, turbidity, and
201 water depth (*H*). All calibration and maintenances follow the YSI, Inc. operating manual
202 methods. Particularly, *chl-a* data were obtained using laboratory calibrated sensors that
203 converts *in vivo* fluorescence of chlorophyll *a* to *chl-a*. The sondes were deployed
204 around 0.5 to 0.9 meters below the surface of the water during the observational
205 period, while the mean water depth *H* was about 2.5 m, and the mean tidal range was
206 about 0.76 m at Station RC. Hourly irradiation data were obtained at nearby Richmond
207 Airport. Also, monthly time series data of surface *chl-a* were collected from Chesapeake
208 Bay Program Long-term Monitoring Stations TF5.4 and TF5.5 (blue squares).

209 The monthly data were used for three long-term timescales (monthly, seasonal, and
210 annual), while the high-frequency data were used to analyze the relative importance of
211 each contribution for continuously increased timescales from hourly to annually.

212 *2.3. Compute relative growth rate*

213 As the instantaneous relative growth rate is defined as $r = \frac{\partial lnB}{\partial t}$, the solution
214 is $B_{t+dt} = B_t e^{r \cdot dt}$ $(dt \to 0)$, which computes biomass measured at time *t* + *dt* (B_{t+dt})
215 from the biomass at time *t* (B_t). This indicates that the relative growth rate can be
216 calculated by the change of biomass. Thus, for a time series of *in situ* measured
217 phytoplankton biomass with an observational time interval of Δt, a time series of
218 relative growth rate $r_{\Delta t}$ that reflects the change in biomass from time *t* to *t* + Δt can be
219 calculated as:

$$r_{\Delta t} = \frac{1}{\Delta t}[\ln(B_{t+\Delta t}) - \ln(B_t)] = \frac{1}{\Delta t}\ln\left(\frac{B_{t+\Delta t}}{B_t}\right) \quad (7)$$

where B_t and $B_{t+\Delta t}$ are the biomass measured at times *t* and *t* + Δt, respectively. For example, $r_{\Delta t}$ is the relative growth rate over daily timescale when $\Delta t = 1$ d; $r_{\Delta t}$ is the relative growth rate over monthly timescale when $\Delta t = 30$ d.

c*hl-a* data were used to obtain phytoplankton biomass. High-frequency *chl-a* data collected at 15-minute intervals were first smoothed to 1-h averages. Using hourly mean c*hl-a* in the units of g m^{-3}, the biomass in the water column can be estimated as $B = C \cdot H = (C{:}\ chl\text{-}a) \cdot chl\text{-}a \cdot H$. Here, the assumption of a well-mixed water column was applied. This assumption is reasonable for the shallow Upper James River with no persistent stratification (Bukaveckas et al., 2011), while the mean euphotic depth is about 2-3 m. For a constant *C: chl-a* ratio (g C/g *chl-a*), the rate can be estimated according to Eq. (7):

$$r_{hr} = \frac{1}{\Delta t}\ln\left[\frac{(chl\text{-}a \cdot H)_{t+\Delta t}}{(chl\text{-}a \cdot H)_t}\right], \text{ with } \Delta t = 1\ hr, \quad (8)$$

where the subscript "*hr*" denotes the observed hourly growth rate, and *C: chl-a* ratio was withdrawn since it did not affect rate computation. The *C: chl-a* ratio varies with seasons and species, which can be measured using observations. We applied a constant *C: chl-a* ratio at Stations TF5.5 and RC as the seasonal variation of *C:chl-a* ratio is relatively small and the average *C: chl-a* ratio was 39±2 g C/g *chl-a* (Bukaveckas et al., 2011).

2.4. Compute transport rate

The transport rate *F* can be computed based on a conservative tracer using a 3D numerical model. For a conservative tracer θ, it is governed by Eq. (1) with zero growth rate (Note that *C* is replaced by tracer concentration θ for clarity):

$$\frac{\partial \theta}{\partial t} + \frac{\partial u\theta}{\partial x} + \frac{\partial v\theta}{\partial y} + \frac{\partial w\theta}{\partial z} = \frac{\partial}{\partial x}\left(K_x \frac{\partial \theta}{\partial x}\right) + \frac{\partial}{\partial y}\left(K_y \frac{\partial \theta}{\partial y}\right) + \frac{\partial}{\partial z}\left(K_z \frac{\partial \theta}{\partial z}\right) \quad (9)$$

where *u*, *v*, *w* represent velocities in the *x*, *y*, and *z* directions, respectively; and K_x, K_y, K_z represent diffusivities in the *x*, *y*, and *z* directions, respectively. For the modeling domain, no tracer comes from the boundaries at all times, i.e. $\theta_{in} = 0$ at both river and open boundaries. By using this boundary condition, it assumes that phytoplankton in the Upper James River are mainly from autochthonous sources, which is reasonable in James River as the *chl-a* at the fall-line of the James River is much lower than the *chl-a* downstream (Bukaveckas et al., 2011). The initial condition, $\theta_0 = 1$, is set everywhere within the domain. The tracer is transported by the dynamic fields, which results in the change of horizontal tracer gradient due to the change of geometry and dynamic forcing conditions. Therefore, the transport rate for tracer concentration, F_θ, can be computed as $F_\theta = -\frac{\partial \theta}{\theta \partial t} = -\frac{\partial ln\theta}{\partial t}$, and the transport rate *F* used in this paper to represent the contribution of transport processes can be computed as $F = -\frac{1}{\int_0^H \theta dz}\frac{\partial \int_0^H \theta dz}{\partial t}$. Because the rate of *F* is normalized by the tracer, the initial condition and the magnitude of the tracer concentration will not affect the model results after a sufficient initial simulation period, and the impact of the initial condition is negligible in the calculation of F.

A real-time three-dimensional numerical model for the James River was developed (Shen et al., 2016) using the Environmental Fluid Dynamics Code (*EFDC*), and it has a good spatial resolution to represent the local variation of complex geometry. The model was forced by hourly tide and salinity at the mouth and hourly wind and heat flux obtained at nearby airport stations, which account for both tidal and meteorological variation. The model was calibrated and verified from 1990–2013 for both hydrodynamics and water quality (Shen et al., 2016). There are a total of 3,066 grid cells in the horizontal and eight layers in the vertical. The model was also used to compute water age in the James River (Shen and Lin, 2006). As the cross-section of the Upper James is narrow and located in the freshwater region without salinity-induced stratification, the volume-controlled freshwater residence time was estimated as the difference of the lateral mean water age at the control section near Stations TF5.4 and TF5.5 along the main channel.

With the use of the numerical model, the transport rate *F* over the entire time series from 2006 to 2008 was computed based on Eq. (9) with specific boundary and initial conditions described above.

2.5. Compute rates for each timescale

Mean rates for timescales longer than the hourly timescale can be obtained by taking the average of the hourly rate r_{hr} over the given time interval of Δt through the following equation:

$$\bar{r} = \frac{1}{\Delta t}\int_t^{t+\Delta t} r_{hr}\,dt = \frac{1}{\Delta t}\int_t^{t+\Delta t} \frac{\partial lnB}{\partial t}\,dt = \frac{1}{\Delta t}\left[\ln(B_{t+\Delta t}) - \ln(B_t)\right] \quad (10)$$

It can be seen that the mean rate only depends on the biomass at the beginning and ending time for the interval of Δt. Therefore, rates for timescales longer than the hourly timescale can be obtained by two equivalent methods, either using Eq. (7) with Δt equals the particular timescale, or using the average as Eq. (10). Here, the two methods Eq. (7) and Eq. (10) were applied to data at Station TF5.5 and RC, respectively. After we obtain both $\bar{r}$ and $\bar{F}$, the effective growth rate $\bar{\mu}$ on that timescale was calculated using Eq. (6), $\bar{\mu} = \bar{r} + \bar{F}$. The overbar will be dropped hereafter when we present results with the understanding that the values are mean values.

2.6. Evaluate contributions of local and transport processes

Eq. (6) provides a way to evaluate the contributions of local processes and transport processes to phytoplankton variability in terms of effective growth rate μ and transport rate *F*. A statistical method is applied to evaluate the contributions of local and transport processes. Correlation coefficient values, R^2, between *F* and *r* and between μ and *r*, are calculated for each timescale to examine the proportions of the variance of *r* that could be explained by *F* and μ, respectively. Additionally, the overall relative importance of local and transport processes on each timescale can be quantified by comparing the root-mean-square (*rms*) of the entire time series of *F* and μ on that timescale:

$$Local: \frac{rms(\mu)}{rms(F)+rms(\mu)};\ Transport: \frac{rms(F)}{rms(F)+rms(\mu)} \quad (11)$$

Note that, on each timescale, the relative importance of each process computed by Eq. (11) used the entire time series of data during the observational period (1990-2013

for Station TF5.5 and 2006-2008 for Station RC); and the analysis reflects their overall contribution during the entire observational period on this timescale, indicating the averaged relative importance or the contribution under normal conditions. The result of short timescale does not represent their contribution over a shorter period during abnormal conditions. For example, episodic events, such as storm surges and large discharge events, may dramatically increase contribution of transport processes in a few days at Station RC, and have greater impact on phytoplankton dynamics than local processes during those events; but these signals were filtered out when considering the entire observational period, and it will later be shown that the change of phytoplankton biomass on daily timescales was overall dominated by local processes (Section 3.7).

3. Results

3.1. Evaluation of contribution of transport processes

By comparing the transport rate to the relative growth rate, the contribution of transport process to phytoplankton biomass variability was evaluated over a sequence of timescales. Note that for long-term timescales (monthly, seasonal, and annual), we only presented results from long-term monitoring data at Station TF5.5, and summarized results from high-frequency data at Station RC at Table 1, and the results from two data sources are comparable.

3.2. Short-term timescales

The correlation of the relative growth rate r and the transport rate F for a 3-year period was analyzed using the high-frequency data for timescales shorter than daily

(Table 1). Overall, their correlations were quite low, suggesting that transport processes were not the dominant processes to phytoplankton variability for those timescales during the observation period.

The tide in this estuary shows a semidiurnal cycle. From a transport perspective, the net effect of transport on biomass is more important in tidal and daily timescales. However, for an intratidal scale, the tide can have a large influence on biomass during the flood and ebb periods, which will modulate the phytoplankton concentration in the water column. The contribution of tide, therefore, is expected to play an important role in the phytoplankton dynamics during food and ebb periods. An example from October 2008 is shown in Fig. 2. Rates r and F on the timescale of 6 h were significantly linearly correlated ($R^2 = 0.52$, $p < 0.001$). The correlation was even higher when only nighttime data were used (Fig. 2c, $R^2 = 0.54$, $p < 0.001$). A strong tidal signal was observed that indicated both rates were modulated by the semidiurnal tide.

The 6-h averaged time series data revealed that increases in phytoplankton biomass occurred during the night ($r > 0$) when no photosynthesis occurred (Fig. 2c), and the mass increase corresponded to a negative transport rate (note that figure plots use $-F$), which suggests that the increases in biomass at night were caused by a "transport in" process due to the transport induced by tides and freshwater discharge. Although the tide can modulate the intratidel transport processes, the large intratidal variability will be filtered for a tidal or daily period and the influence of net physical transport processes on biomass on tidal and daily timescales is not as important as local processes (Table 1).

3.3. Monthly timescale

The time series of *chl-a* and local residence time for the period of 2000-2013 at Station TF5.5 is plotted in Fig. 3a. This figure shows that *chl-a* and residence time had the same variations. On a monthly timescale, *chl-a* correlated with the residence time ($R^2 = 0.33$, $p < 0.001$, Fig. 3b). Lower *chl-a* was shown to correspond with shorter residence time, though the correlation was more diverse when residence time was long, which usually occurred in the summer, indicating that the contribution of local processes is more important during summer when the dynamic conditions become favorable for growth.

The transport rate *F* was correlated to the relative growth rate *r* at Station TF5.5 for the period from 2000 to 2013 ($R^2 = 0.25$, $p < 0.001$) as shown in Fig. 3c and 3d. Variations of *r* and *F* were in phase, in general, which suggests that the monthly variability of phytoplankton biomass is modulated by hydrodynamics. Note that only 13-year result was presented in Fig. 3 for making the plot clear, and the correction between *r* and *F* during the entire years of long-term monitoring data (1990-2013) was shown in Table 1.

3.4. Seasonal timescale

For the seasonal timescale, analysis of the time-series data from the years 1990 to 2013 showed that transport rate *F* was correlated with relative growth rate *r* ($R^2 = 0.22$, $p < 0.001$, Fig. 4b). The transport rate *F* remained positive, and transport processes had a net “transport out” effect on phytoplankton biomass throughout the observation period (Fig. 4a). The relative growth rate *r* had either positive or negative values, but the

365 corresponding effective growth rate μ was always positive, suggesting that the
366 contribution of local processes leads to an increase in phytoplankton biomass.

367 All three rates (*r*, *F*, and μ) showed seasonal variations (Fig. 5). The transport rate, *F*,
368 appeared to have smaller magnitudes during summer than during other seasons,
369 corresponding to the lowest freshwater discharge into the James River in the summer.
370 The effective growth rate, μ, seemed to be lower during summer and fall than during
371 spring and winter. This seasonal change can be attributed to a change in composition of
372 algal species and an increase in respiration, grazing, and nutrient limitation during the
373 summer (Marshall and Egerton, 2013). As a consequence, the relative growth rate
374 tended to be low during summer and fall, even though *F* was lower. It shows that μ was
375 much larger than *r*, after removal of the impact of transport processes (Fig. 5), indicating
376 the values of *r* would underestimate the effective growth rate of phytoplankton without
377 considering any effect of the physical transport.

378 *3.5. Annual timescale*

379 For the annual timescale, the correlation between *F* and *r* was significant ($R^2 = 0.48$, p
380 < 0.001, Fig. 4b) and it was higher than the correlation between μ and *r* ($R^2 = 0.24$, $p <$
381 0.001). Similar to the seasonal timescale, both *F* and μ remained positive, while the
382 magnitude of the relative growth rate *r* diminished (Fig. 4c), indicative of the balance
383 between local and transport processes. The contribution of transport processes showed
384 a net "transport out" effect on interannual phytoplankton biomass variability in the
385 Upper James River, i.e. more biomass was transported out of this region than was
386 transported in.

3.6. Rate variations

The daily effective growth rate, μ, may be of the same magnitude as the gross growth rate, *G*, if respiration and grazing pressure are very low. Theoretically, the daily gross growth rate represents photosynthetic production, and it has maximum values ranging from 1 to 5 d^{-1} dependent on the temperature, nutrients, and phytoplankton species (Eppley, 1972; Brush et al., 2002). However, the estimated effective growth rate may be an order of magnitude smaller than the theoretical maximum values, due to suppression of photosynthesis by nutrient and light limitation, respiration, settling, and grazing. The variability of μ reflects a net response of phytoplankton to the change of local environment conditions.

We used median rates as representative of typical values for each timescale (Fig. 6a). Positive values of the rates *r*, μ and *–F* corresponded to the increase of phytoplankton biomass whereas negative values indicated a decrease. Both medians of positive and negative rates, respectively, are listed in Table 1. In general, both the medians of positive and negative rates decreased as the timescale increased.

For seasonal or longer timescales, the medians of transport rates (*-F*) were negative at Station RC (Table 1). In fact, *-F* was always negative on these long-term timescales, suggesting that the net contribution of transport processes flushed biomass downstream ("transport out"). μ was always positive, suggesting that the net contribution of local processes was to increase the phytoplankton biomass, i.e., phytoplankton primary production was larger than the loss from respiration, excretion, settling, and grazing. The competition between local and transport processes leads to

409 either an increase or a decrease of phytoplankton biomass, which was reflected by the
410 existence of both positive and negative values of *r* when the timescale exceeded the
411 monthly timescale.

412 *3.7. Relative importance of local and transport processes*

413 The increased correlation between rates *F* and *r* from a monthly timescale to an
414 annual timescale, based on analysis of long-term monthly monitoring data at Station
415 TF5.5, suggested that the relative importance of the transport processes to
416 phytoplankton variability increases when evaluating it on a longer timescale. This result
417 was consistent with the evaluation using high-frequency data at Station RC during 2006
418 to 2008 (Fig. 6c and 6d). The coefficient of determination, R^2, also showed that the
419 proportions of *r* variance that could be explained by the transport rate *F* increased with
420 the increase of timescale, whereas the proportions that could be explained by the
421 effective growth rate, μ, decreased.

422 The relative importance of contributions of local and transport processes over
423 continuously increasing timescales were compared for the period from 2006 to 2008
424 (Fig. 6d). The relative importance of transport processes had an increasing trend with
425 increasing timescale whereas that of local processes had a decreasing trend, and they
426 were equally important in the monthly timescale at Station RC. The relative importance
427 of each contribution was more diverse in timescales shorter than daily; it shows that the
428 contribution of local processes peaked on daily and tidal timescales, whereas the
429 transport processes showed peaked relative importance on timescales around 6 and 18
430 h (Fig. 6d). These variations are caused by the intratidal variability and will be discussed

in the next section. It can be seen that tide also modulates the local processes though the net tidal contribution is less.

4. Discussion

4.1. Factors affecting local and transport processes

Similar to the hydrodynamic conditions investigated for many other estuaries (Wang et al., 2004; Barcena et al., 2012; Lemagie and Lerczak, 2015), river inflow and tides are the two primary factors affecting the transport processes in the Upper James River and contribute to phytoplankton biomass dynamics, while other forcings such as wind play less important roles.

River inflow determines the overall net long-term advection characteristics of the Upper James River. The phytoplankton biomass transported from the upstream freshwater is generally found to be smaller than the biomass generated in the tidal freshwater region and estuary (e.g., Bukaveckas et al., 2011; Peierls et al., 2012; Paerl et al., 2014). As the residual current always flows downstream, the biomass is transported downstream, resulting in a net "transport out" effect on phytoplankton biomass when viewing it from a long-term perspective. Consistently, river inflow also had the net "transport out" effect in the Upper James River, reflected by only positive medians of transport rate *F* found on the annual timescale (Table 1).

Tides also have substantial effects on phytoplankton variability. The dominant constituent of tide in the Upper James River is the semi-diurnal M_2 tide with a 12.42-h tidal period. Both advective and diffusive transport are enhanced during either flood or

ebb tides, which increase the relative importance of transport processes on a timescale of about one-half of the tidal period (around 6 h); whereas the largest relative importance of local processes is around tidal and daily timescales, because the net impact on transport processes from tides is minimal by averaging over a complete tidal cycle, it is consistent with results in Fig. 6c and d.

The local processes are fundamental for phytoplankton variability, regardless of the transport processes. It is found that local processes always have an important contribution to the phytoplankton biomass dynamics in the Upper James River even on the timescales with a large physical contribution (Fig. 6d). For the monthly timescale, the results are more scattered with an increase of residence time (Fig. 3b), these large residence times usually occurred in summers when both riverine flows and transport rate were small (Fig. 5), and the contribution of local processes became relatively more important than that of transport processes. Local processes play critical roles on diurnal timescales, owing to the well-recognized diurnal variation that phytoplankton biomass increases during the day because of photosynthesis, but decreases at night.

The contribution of local processes also showed seasonal variations represented by the effective growth rate μ (Fig. 5). In general, a smaller value of μ appeared in summer and fall than during winter and spring. One possible reason for this seasonal change is the phytoplankton species succession. The “transport out” effect by freshwater has been found to be a determining factor on phytoplankton growth and composition in river-dominated estuaries as it tends to select fast-growing species in high-flow conditions (Ferreira et al., 2005; Paerl et al., 2006; Costa et al., 2009). The maximum

freshwater discharge occurs in the winter and spring in the James River. The enhanced "transport out" processes along with abundant nutrients favors freshwater diatoms that have relatively high intrinsic growth rates to become the dominant species in these two seasons. In the summer and fall, when the "transport out" effect is reduced and residence time increases, the percentage contribution of dinoflagellates and cyanobacteria with lower intrinsic growth rates increases (Valdes-Weaver et al., 2006; Marshall and Egerton, 2013). Temperature, nutrients, and grazing may be other factors affecting the seasonal change of the contribution of local biological processes, as respiration and grazing often peak in summer while nutrient limitation is severe though with large benthic flux input of recycled nutrients (Kemp et al., 2005).

4.2. Long-term validation

Complex phytoplankton dynamics can be described by the balance between local and transport processes under steady-state conditions (Lucas et al., 2009), and it is expected that this balance is acceptable on long-term timescales but may be questionable on shorter timescales. Therefore, it is interesting to examine on which timescales this assumption is valid.

The steady-state assumption is equivalent to assuming that $r = 0$, or that the magnitude of r is negligible compared to the magnitudes of μ and F. Direct comparisons of r to μ and F show that the assumption is valid for seasonal to annual timescales in the region as r is small. By using the root-mean-square (*rms*) of each rate to quantify their magnitudes, it is found that the ratios of *rms*(F) to *rms*(r) and *rms*(μ) to *rms*(r) increased as timescales increased (Fig. 6b). This suggests that contributions of local and

transport processes have the tendency to be balanced only when the timescale is longer than 10 days (Fig. 6a and b). Their difference becomes more significant for hourly to daily timescales.

4.3. Phytoplankton primary production

The open water method using high-frequency dissolved oxygen data has been widely applied to estimate gross primary production, ecosystem respiration, and net ecosystem metabolism (Staehr et al., 2012). Because of the influence of advection processes, high-frequency phytoplankton data have not often been used to estimate these metabolic rates. Here, we used high-frequency *chl-a* data to estimate phytoplankton gross primary productivity similar to open water oxygen method and to evaluate the influence of physical transport on estimation of the rate.

For each time interval (e.g. Δt = 15 minutes), the change of phytoplankton biomass (ΔB) is described by the equation below:

$$\frac{\Delta B}{\Delta t} = GPP - RPP - FPP \quad (12)$$

where *GPP* is the 15-minute phytoplankton gross primary productivity (g C m^{-2} 15 min^{-1}), *RPP* is the 15-minute rate of total phytoplankton respiration and consumption (including respiration, grazing, and settling, g C m^{-2} 15 min^{-1}), which represents total biological losses. *FPP* is the 15-minute rate of transport in or out of phytoplankton by transport processes (g C m^{-2} 15 min^{-1}); a positive *FPP* (-*F* < 0) means that the carbon produced by local biological processes is transported out of this location and benefits the food web in

adjacent areas (Cloern, 2007). We also use *DPP* to denote the difference between *GPP* and *RPP*,

$$DPP = GPP - RPP. \quad (13)$$

FPP is estimated from the product of phytoplankton biomass and transport rate, and it was calculated using the transport rate *F* computed from the numerical model in this study ($FPP = F \cdot B$). The method for computing *GPP* and *RPP* is similar to the open water method, and *DPP* was first computed by summation of $\Delta B/\Delta t$ and *FPP* for each time interval. Daily *RPP* was estimated from the extrapolation of nighttime *RPP* (= the sum of nighttime 15-minute *DPP*) to one day; and daily *GPP* was estimated, according to Eq. (13), from daily *DPP* (= the sum of 15-minute *DPP* over one day) plus daily *RPP*. Both daily GPP and RPP are in units of g C m^{-2} d^{-1}. Unrealistic negative values of daily *GPP* were found for some days (about 24%), and they were excluded from the calculations following the way of the open water method (Caffrey, 2003). Most of the negative daily *GPP* values appeared on rainy days when precipitation may enhance the flushing effect from runoff from adjacent watersheds. The results are representative of primary productivity and metabolic rates under normal weather conditions. Note that the transport rate *F* used was computed from the numerical model that only represents the physical transport as shown in Eq. (6), and the results are only used to quantify the influence of physical transport on the estimation of *GPP*.

For the Upper James River, the typical *C*: *chl-a* ratio equals 39 g C/g *chl-a* with small seasonal variability (Bukaveckas et al., 2011). Because we have no winter data, the

annual phytoplankton primary production cannot be correctly estimated. Nevertheless, we assumed that gross primary production in winter was lower than or equal to the minimum of seasonal production. The annual phytoplankton gross primary production were estimated to be about 255.90, 685.91, and 486.26 g C m^{-2} yr^{-1}, respectively, for the years 2006, 2007, and 2008 (Table 2). These estimations were comparable to the 12-year averaged (1989-2001) annual phytoplankton gross primary production, around 230 g C m^{-2} yr^{-1}, measured in the laboratory using ^{14}C method at Station TF5.5 (Nesius et al., 2007). An example of the seasonal averages of *GPP*, *RPP*, and *DPP* in 2008 are also shown (Fig. 7), and the seasonal average of *GPP* during the summer 2008 was 2.31 g C m^{-2} d^{-1}, close to the seasonal mean rate of 2.11 g C m^{-2} d^{-1} using the method of dissolved oxygen incubations for the nearby York River during the same time period (Lake et al., 2013).

The amount of primary production transported out ranges from 7% to 13% (*FPP*/*GPP*). It suggests that the net physical transport processes have a minor impact on estimates of *GPP* and *RPP* on daily scale under normal weather conditions. This is consistent with the analysis of biomass variability on the daily timescale.

5. Conclusions

To evaluate the contribution of transport processes to phytoplankton biomass variability using high-frequency observational data, we introduced the transport rate method, which enables us to estimate each contribution exclusively as a first-order approximation. The Upper James River was selected as the study site, and the results

556 support the hypothesis that both local and transport processes contributed significantly
557 to the local variability of phytoplankton biomass, but their relative importance changed
558 on different timescales. On a short-term basis such as daily and weekly timescales, even
559 though the transport processes could modulate phytoplankton biomass variability on an
560 intratidal timescale due to flood and ebb variations, the intratidal variations will be
561 removed over a tidal cycle. The local processes dominated the overall contributions
562 during the observational period; however, the relative importance of transport
563 processes tended to be equivalent to the local processes in the long-term timescales
564 (e.g., seasonal and annual). Another analysis of this study shows that the local processes
565 were almost balanced by the transport process on the seasonal and annual timescales,
566 and approached a steady-state condition for phytoplankton dynamics, whereas the time
567 derivative term became important for shorter timescales.

568 Examination of the transport rate revealed that transport processes exhibited a
569 persistent “transport out” effect on long-term timescales to decrease *in situ*
570 phytoplankton biomass in this region, but it was not the case for timescales shorter than
571 seasonal that transport processes could either increase or decrease the biomass,
572 corresponding to “transport in” and “transport out” processes, respectively.

573 Transport processes had a small impact on the estimation of daily gross
574 phytoplankton productivity. By applying a method analogous to the open water oxygen
575 method that calculates phytoplankton gross primary production using 15-minute
576 observational data, the percentage of production flushed out was around 7-13% under
577 normal weather conditions.

The use of the transport rate is a first-order approximation for quantifying transport processes. Zero concentrations were applied at the boundaries for this study, and the computed transport rate *F* did not account for the possible effects of inputs from boundaries (though these are very low), and therefore the contribution of the transport processes considered was the redistribution of biomass produced within the study area due to the change of dynamics and geometry. The additional bias of the transport rate on the hourly timescale could come from the numerical method and model grid resolution that may not be able to simulate the microscale varibility of physical processes, which causes the patchiness of phytoplankton distribution that makes the observed *chl-a* data fluctuate highly with a change of dynamic conditions. Besides the use of the numerical calculation, the transport rate can also be estimated based on field observations of current, salinity and water depth. In addition, the pattern of the relative importance of local and transport processes on different timescales demonstrated in the Upper James River may vary at other locations of the estuary, which would warrant further study.

Acknowledgments

The funding of this study was supported by the Virginia Institute of Marine Science and the Virginia Department of Environmental Quality. We are thankful to Mark J. Brush for his critical review of the manuscript and invaluable suggestions. We also thank Marjy A.M. Friedrichs, and Kyeong Park for their comments and suggestions. We are grateful to Mac Sisson for help editing the manuscript. We thank two anonymous reviewers for their constructive comments that helped us to improve the manuscript. This is

599 Contribution No. 3645 of the Virginia Institute of Marine Science, College of William and
600 Mary.

References

601 Bárcena, J.F., García, A., Gómez, A.G., Álvarez, C., Juanes, J.A. and Revilla, J.A., 2012.
602 Spatial and temporal flushing time approach in estuaries influenced by river and tide. An
603 application in Suances Estuary (Northern Spain). Estuarine, Coastal and Shelf
604 Science, 112, 40-51.

605 Brush, M.J., Brawley, J.W., Nixon, S.W. and Kremer, J.N., 2002. Modeling phytoplankton
606 production: problems with the Eppley curve and an empirical alternative. Marine
607 Ecology. Progress Series, 238, 31-45.

608 Bukaveckas, P.A., Barry, L.E., Beckwith, M.J., David, V. and Lederer, B., 2011. Factors
609 determining the location of the chlorophyll maximum and the fate of algal production
610 within the tidal freshwater James River. Estuaries and Coasts, 34(3), 569-582.

611 Caffrey, J.M., 2003. Production, respiration and net ecosystem metabolism in US
612 estuaries. Environmental Monitoring and Assessment, 81, 207-219.

613 Caffrey, J.M., 2004. Factors controlling net ecosystem metabolism in US
614 estuaries. Estuaries, 27(1), 90-101.

615 Chapra, S.C., 1997. Surface Water-Quality Modeling. McGraw Hill, New York, NY.

616 Cloern, J.E., 2001. Our evolving conceptual model of the coastal eutrophication
617 problem. Marine Ecology Progress Series, 210, 223-253.

618 Cloern, J.E., 2007. Habitat connectivity and ecosystem productivity: Implications from a
619 simple model. The American Naturalist, 169(1), E21-E33.

620 Cole, J.J., Pace, M.L., Carpenter, S.R., and Kitchell, J.F., 2000. Persistence of net
621 heterotrophy in lakes during nutrient addition and food web manipulations Limnology
622 and Oceanography, 45, 1718-1730.

623 Costa, L.S., Huszar, V.L.M. and Ovalle, A.R., 2009. Phytoplankton functional groups in a
624 tropical estuary: hydrological control and nutrient limitation. Estuaries and
625 Coasts, 32(3), 508-521.

626 Eppley, R.W., 1972. Temperature and phytoplankton growth in the sea. Fisheries
627 Bulletin, 70(4), 1063-1085.

628 Ferreira, J.G., Wolff, W.J., Simas, T.C. and Bricker, S.B., 2005. Does biodiversity of
629 estuarine phytoplankton depend on hydrology?. Ecological Modelling, 187(4), 513-523.

630 Howarth, R., and Michaels, A.F., 2000. The measurement of primary production in
631 aquatic ecosystems, p. 72–85. In O. Sala, R. Jackson, H. Mooney, and R. W. Howarth
632 [eds.], Methods in ecosystem science. Springer-Verlag.

633 Kemp, W.M. and Boynton, W.R., 1980. Influence of biological and physical processes on
634 dissolved oxygen dynamics in an estuarine system: implications for measurement of
635 community metabolism. Estuarine and Coastal Marine Science, 11(4), 407-431.

636 Kemp, W.M. and Testa, J.M., 2011. Metabolic balance between ecosystem production
637 and consumption. Treatise on estuarine and coastal science, 7.

638 Kemp, W.M., Boynton, W.R., Adolf, J.E., Boesch, D.F., Boicourt, W.C., Brush, G.,
639 Cornwell, J.C., Fisher, T.R., Glibert, P.M., Hagy, J.D. and Harding, L.W., 2005.
640 Eutrophication of Chesapeake Bay: historical trends and ecological interactions. Marine
641 Ecology Progress Series, 303, 1-29.

642 Kremer, J.N. and Nixon, S.W., 1978. Coastal marine ecosystem: simulation and analysis.
643 In Coastal marine ecosystem: simulation and analysis. Springer-Verlag.

644 Lake, S.J., Brush, M.J., Anderson, I.C., and Kator, H.I., 2013. Internal versus external
645 drivers of periodic hypoxia in a coastal plain tributary estuary: the York River, Virginia.
646 Marine Ecology Progress Series 492:21-39.

647 Lancelot, C. and Muylaert, K., 2011. Trends in estuarine phytoplankton ecology. In:
648 Wolanski, E., et al. (Eds.), Treatise on Estuarine and Coastal Science, Functioning
649 Ecosystems at the Land-ocean Interface, vol. 7, 5-15.

650 Lemagie, E.P. and Lerczak, J.A., 2015. A comparison of bulk estuarine turnover
651 timescales to particle tracking timescales using a model of the Yaquina Bay
652 Estuary. Estuaries and Coasts, 38(5), 1797-1814.

653 Lucas, L.V., Koseff, J.R., Monismith, S.G., Cloern, J.E. and Thompson, J.K., 1999.
654 Processes governing phytoplankton blooms in estuaries. II: The role of horizontal
655 transport. Marine Ecology Progress Series, 187, 17-30.

Lucas, L.V., Sereno, D.M., Burau, J.R., Schraga, T.S., Lopez, C.B., Stacey, M.T., Parchevsky, K.V. and Parchevsky, V.P., 2006. Intradaily variability of water quality in a shallow tidal lagoon: mechanisms and implications. Estuaries and Coasts, 29(5), 711-730.

Lucas, L.V., Thompson, J.K. and Brown, L.R., 2009. Why are diverse relationships observed between phytoplankton biomass and transport time. Limnology and Oceanography, 54(1), 381-390.

Marshall, H.G. and Egerton, T.A., 2013. Assessing seasonal relationships between chlorophyll a concentrations to phytoplankton composition, biomass, and abundance, emphasizing the bloom producing algae (HAB and others) within the James, Elizabeth, and Lafayette Rivers in Virginia.

Nesius, K.K., Marshall, H.G. and Egerton, T.A., 2007. Phytoplankton Productivity in the Tidal Regions of Four Chesapeake Bay (USA) Tributaries. Virginia Journal of Science, 58(4).

Odum, H.T., 1956. Primary production in flowing waters. Limnology and Oceanography, 1(2), 102-117.

Paerl, H.W., Hall, N.S., Peierls, B.L., Rossignol, K.L. and Joyner, A.R., 2014. Hydrologic variability and its control of phytoplankton community structure and function in two shallow, coastal, lagoonal ecosystems: the Neuse and New River Estuaries, North Carolina, USA. Estuaries and Coasts,37(1), 31-45.

675 Paerl, H.W., Valdes, L.M., Peierls, B.L., Adolf, J.E. and Harding Jr, L.W., 2006.
676 Anthropogenic and climatic influences on the eutrophication of large estuarine
677 ecosystems. Limnology and Oceanography, 51(1 part 2), 448-462.

678 Peierls, B.L., Hall, N.S. and Paerl, H.W., 2012. Non-monotonic responses of
679 phytoplankton biomass accumulation to hydrologic variability: a comparison of two
680 coastal plain North Carolina estuaries. Estuaries and Coasts, 35(6), 1376-1392.

681 Reaugh, M.L., Roman, M.R. and Stoecker, D.K., 2007. Changes in plankton community
682 structure and function in response to variable freshwater flow in two tributaries of the
683 Chesapeake Bay. Estuaries and Coasts, 30(3), 403-417.

684 Shen, J. and Lin, J., 2006. Modeling study of the influences of tide and stratification on
685 age of water in the tidal James River. Estuarine, Coastal and Shelf Science, 68(1), 101-
686 112.

687 Shen, J., Wang, T., Herman, J., Mason, P. and Arnold, G.L., 2008. Hypoxia in a coastal
688 embayment of the Chesapeake Bay: A model diagnostic study of oxygen
689 dynamics. Estuaries and Coasts, 31(4), 652-663.

690 Shen, J., Wang, Y. and Sisson, M., 2016. Development of the Hydrodynamic Model for
691 Long-Term Simulation of Water Quality Processes of the Tidal James River,
692 Virginia. Journal of Marine Science and Engineering, 4(4), p.82.

693 Staehr, P.A., Bade, D., Van de Bogert, M.C., Koch, G.R., Williamson, C., Hanson, P., Cole,
694 J.J. and Kratz, T., 2010. Lake metabolism and the diel oxygen technique: state of the
695 science. Limnology and Oceanography: Methods, 8(11), 628-644.

696 Staehr, P.A., Testa, J.M., Kemp, W.M., Cole, J.J., Sand-Jensen, K., and Smith, S.V., 2012.
697 The metabolism of aquatic ecosystems: history, applications, and future challenges.
698 Aquat. Sci. 74, 15-29.

699 Valdes-Weaver, L.M., Piehler, M.F., Pinckney, J.L., Howe, K.E., Rossignol, K. and Paerl,
700 H.W., 2006. Long‐term temporal and spatial trends in phytoplankton biomass and
701 class‐level taxonomic composition in the hydrologically variable Neuse‐Pamlico
702 estuarine continuum, North Carolina, USA. Limnology and Oceanography, 51(3), 1410-
703 1420.

704 Wang, C.F., Hsu, M.H. and Kuo, A.Y., 2004. Residence time of the Danshuei River
705 estuary, Taiwan. Estuarine, Coastal and Shelf Science, 60(3), 381-393.

706 Table 1. Estimated values for each parameter for different timescales based on analysis of three years of high-frequency continuous
707 monitoring data at Station JMS073.37 (RC) and 24 years of long-term monitoring data at Station TF5.5 (1990-2013). Results of
708 transport rate *F* are computed from the 3D numerical model.

Statistical parameters for each timescales	**Continuous Monitoring Station (JMS073.37) 2006 – 2008**							**Long-term Monitoring Station (TF5.5) 1990 – 2013**		
	Hourly (1 h)	**Tidal** (12.5 h)	**Daily** (1 d)	**Spring-neap** (14.5 d)	**Monthly** (30 d)	**Seasonal** (90 d)	**Annual** (365 d)	**Monthly**	**Seasonal**	**Annual**
Medians of (d^{-1})										
positive r	1.3795	0.2437	0.1059	0.0217	0.0106	0.0047	0.0014	0.0246	0.0148	0.0042
negative r	-1.2740	-0.2443	-0.1112	-0.0245	-0.0128	-0.0073	-0.0042	-0.0213	-0.0112	-0.0027
positive -F	1.3174	0.1359	0.0564	0.0106	0.0210	/	/	0.0184	/	/
negative -F	-1.1343	-0.1481	-0.0740	-0.0328	-0.0319	-0.0391	-0.0406	-0.0421	-0.0469	-0.0479
positive μ	1.3555	0.2987	0.1402	0.0461	0.0379	0.0379	0.0369	0.0472	0.0482	0.0496
negative μ	-1.3179	-0.2779	-0.1293	-0.0185	-0.0107	/	/	-0.0161	/	/
Correlation of determination R^2										
$F \sim r$	0.0138	0.0011	0.0071	0.1082	0.1503	0.4612	0.6106	0.1687	0.2172	0.4755
$\mu \sim r$	0.9226	0.7921	0.7184	0.2843	0.2148	0.0768	0.0211	0.5750	0.5137	0.0275
Relatively Importance										
Transport	0.2189	0.3148	0.3509	0.4947	0.5067	0.5207	0.5172	0.5258	0.5081	0.4910
Local	0.7811	0.6852	0.6491	0.5053	0.4933	0.4793	0.4828	0.5485	0.5159	0.5103

709

710 Table 2. Estimates of annual phytoplankton gross primary production (*GPP*), total
711 biological losses (*RPP*, including respiration, grazing and settling), *DPP* (*GPP* - *RPP*), the
712 amount of production flushed out (*FPP*) at Station RC for the three years 2006 to 2008.
713 *FPP*/*GPP* representing the fraction of production flushed out are also presented.

Annual phytoplankton metabolic rates	***GPP*[1]**	***RPP*[1]**	***DPP*[1]**	***FPP*[2]**	$\frac{FPP}{GPP}$
	(g C m^{-2} yr^{-1})				
2006	255.90	274.29	-18.39	32.65	12.76%
2007	685.91	688.50	-2.59	47.76	6.96%
2008	486.26	512.42	-26.16	31.87	6.55%

[1]estimated using 15-minute observational data
[2]estiatmed using numerical model

714

Figure Captions

Fig. 1. Map of the Chesapeake Bay and James River. Locations for the Continuous Monitoring Stations RC, and the Long-term Monitoring Stations TF5.4 and TF5.5 are shown, respectively, by the green triangle and the blue squares. The domain of the James River 3D model is also presented.

Fig. 2. Comparison of the 6-h moving averages of *r* and *F* at Station RC in October 2008. a) time series of relative growth rate *r* (red line), transport rate *F* (blue line, here plotted as –*F*), and irradiance (black line); b) the relation between -*F* and *r* using all data during the month (daytime + nighttime); c) the relation between -*F* and *r* only at nighttime.

Fig. 3. Contributions of transport processes on monthly timescales at Station TF5.5. a) time series of *chl-a* (black line, $\mu g\ L^{-1}$) and residence time (blue line); b) the relationship between *chl-a* and residence time; c) time series of relative growth rate *r* (black line) and transport rate *F* (blue line, –*F*); d) the relationship between -*F* and *r*. The data used are from the years 2000 to 2013.

Fig. 4. Rates *r*, -*F*, and μ on seasonal and annual timescales during the years 1990 to 2013 at Station TF5.5.

Fig. 5. Box plot for rates *r*, -*F*, and μ on seasonal timescale during the years 1990 to 2013 at Station TF5.5. Horizontal lines in the boxes indicate medians, boxes indicate interquartile ranges, whiskers indicate the extremes that are set to be 1.5 times the range from the boxes, notches in boxes indicate the 95% confidence intervals of medians, and circles indicate outliers.

735 Fig. 6. a) Medians over different timescales for positive and negative rates, respectively.
736 Transport rate (–*F*, blue lines), relative growth rate *r* (red lines), and growth rate
737 μ (green lines); b) Ratios of root-mean-square of rates. Blue line denotes *rms*(*F*) to
738 *rms*(*r*), green line denotes *rms*(μ) to *rms*(*r*); c) coefficient of determination R^2 between *F*
739 and *r* (blue line) and between μ and *r* (green line); and d) estimates of the relative
740 importance of transport processes (blue line) and local processes (green line).

741 Fig. 7. Phytoplankton primary production in each season of 2008 at Station RC, by
742 assuming $FPP = F \cdot B$ (winter data are not available). Phytoplankton gross primary
743 productivity (*GPP*), phytoplankton total biological losses (*RPP*, including respiration,
744 grazing and settling), phytoplankton *DPP* (*GPP* - *RPP*), error bars represent the 95%
745 confidence intervals.

746

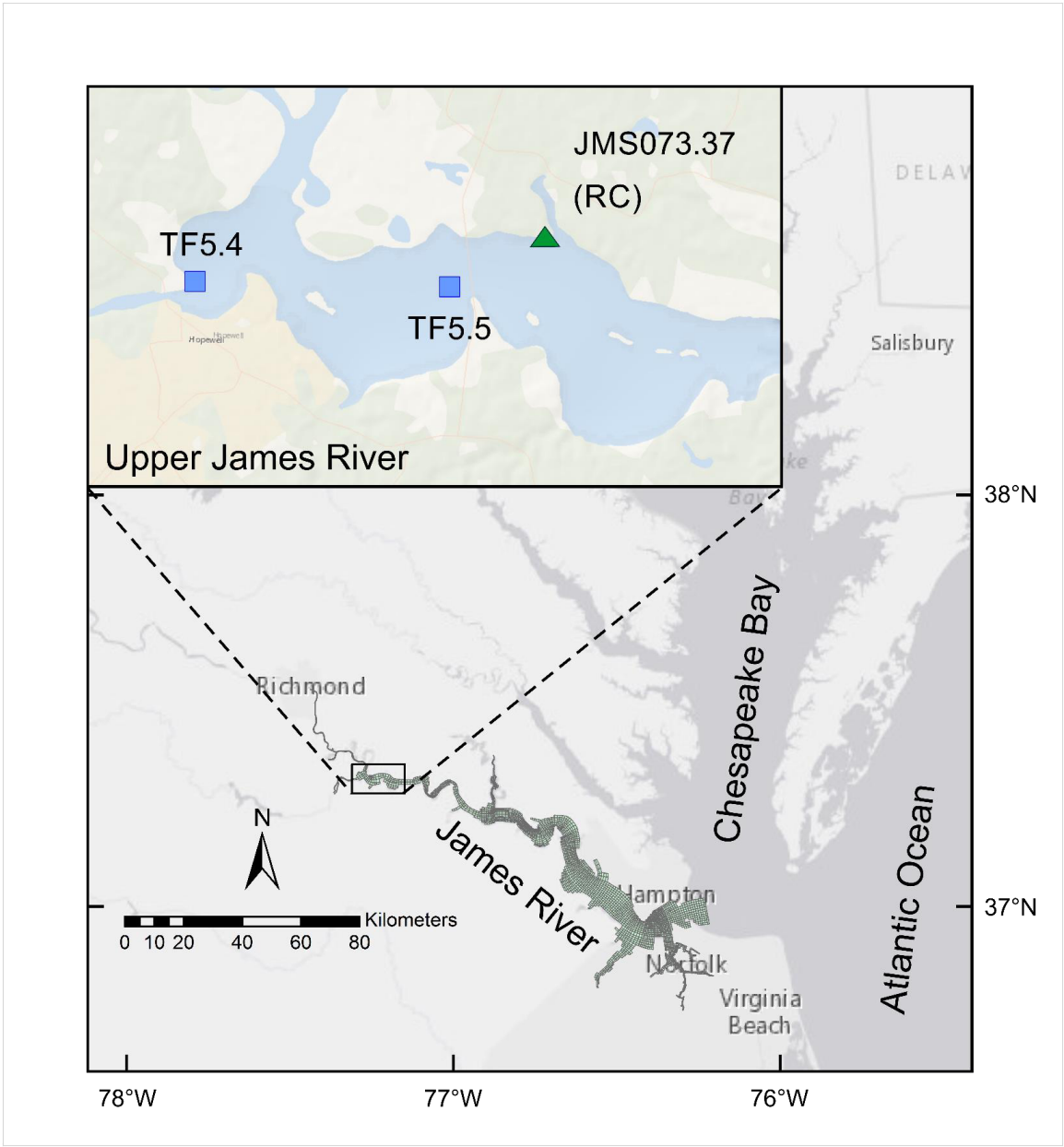

747

748 Fig. 1. Map of the Chesapeake Bay and James River. Locations for the Continuous

749 Monitoring Stations RC, and the Long-term Monitoring Stations TF5.4 and TF5.5 are

750 shown, respectively, by the green triangle and the blue squares. The domain of the

751 James River 3D model is also presented.

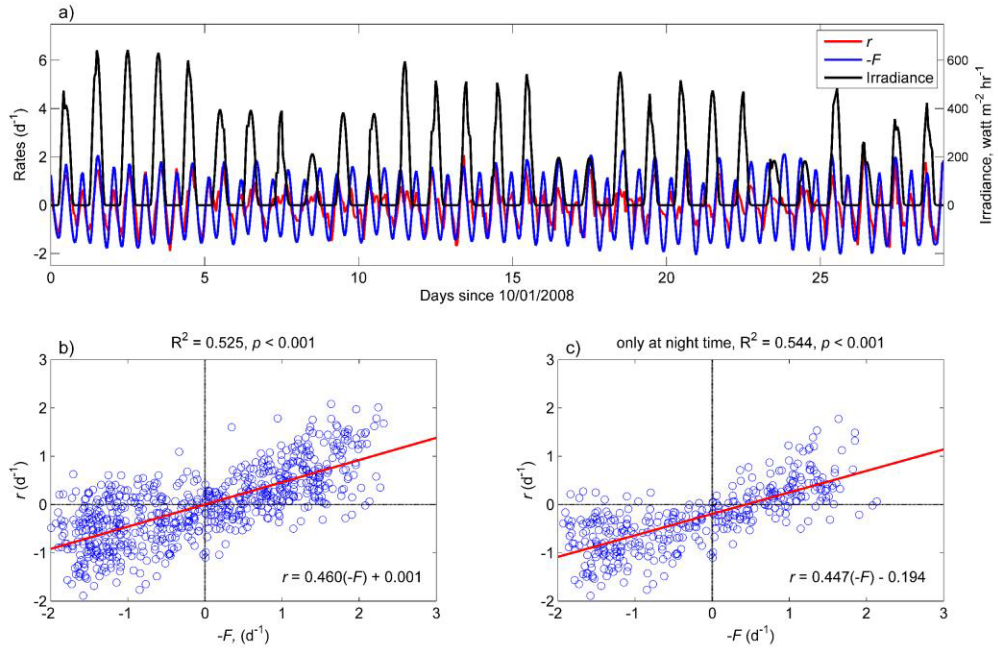

752

753 Fig. 2. Comparison of the 6-h moving averages of *r* and *F* at Station RC in October 2008.

754 a) time series of relative growth rate *r* (red line), transport rate *F* (blue line, here plotted

755 as –*F*), and irradiance (black line); b) the relation between -*F* and *r* using all data during

756 the month (daytime + nighttime); c) the relation between -*F* and *r* only at nighttime.

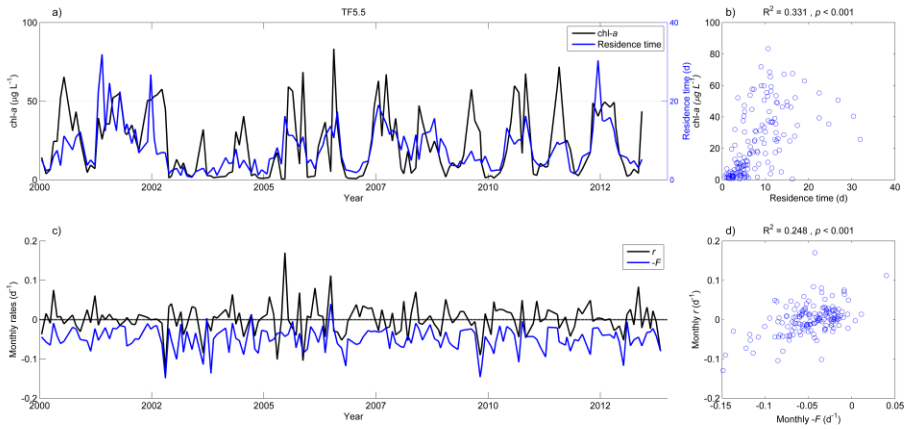

757

758 Fig. 3. Contributions of transport processes on monthly timescales at Station TF5.5. a)

759 time series of *chl-a* (black line, $\mu g\ L^{-1}$) and residence time (blue line); b) the relationship

760 between *chl-a* and residence time; c) time series of relative growth rate *r* (black line)

761 and transport rate F (blue line, *–F*); d) the relationship between *-F* and *r*. The data used

762 are from the years 2000 to 2013.

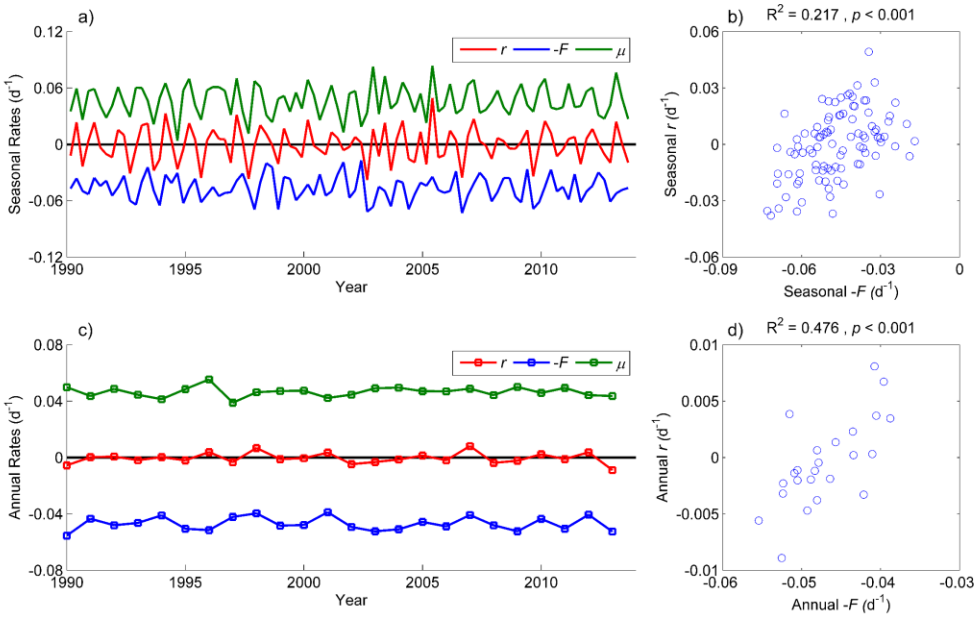

763

764 Fig. 4. Rates *r*, *-F*, and μ on seasonal and annual timescales during the years 1990 to

765 2013 at Station TF5.5.

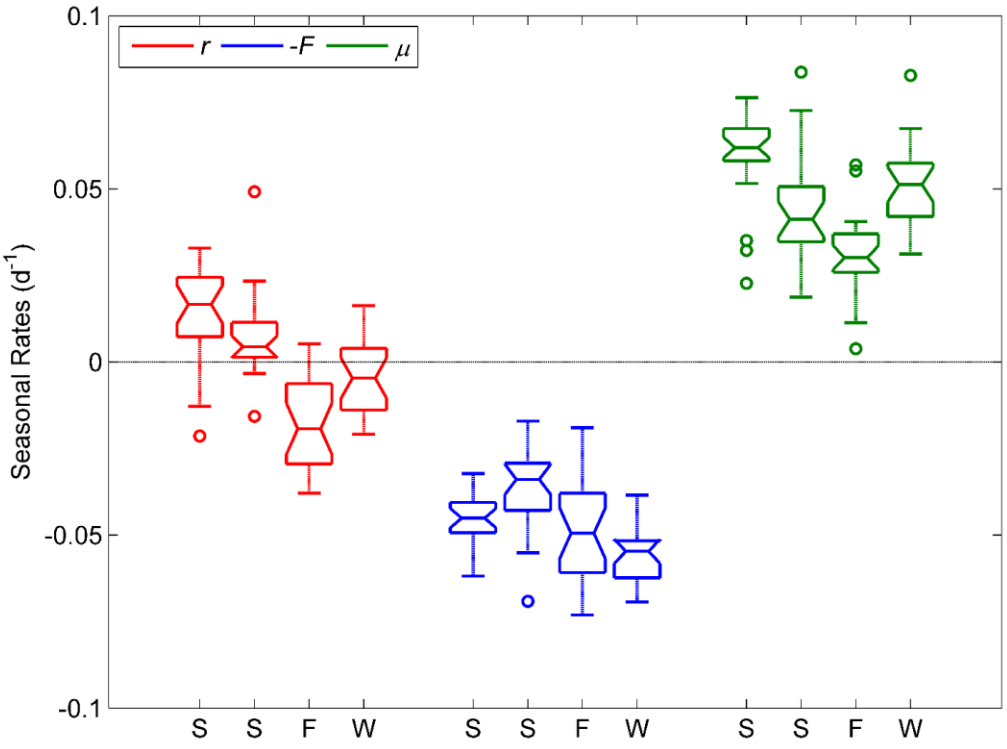

766

767 Fig. 5. Box plot for rates *r*, *-F*, and μ on seasonal timescale during the years 1990 to

768 2013 at Station TF5.5. Horizontal lines in the boxes indicate medians, boxes indicate

769 interquartile ranges, whiskers indicate the extremes that are set to be 1.5 times the

770 range from the boxes, notches in boxes indicate the 95% confidence intervals of

771 medians, and circles indicate outliers.

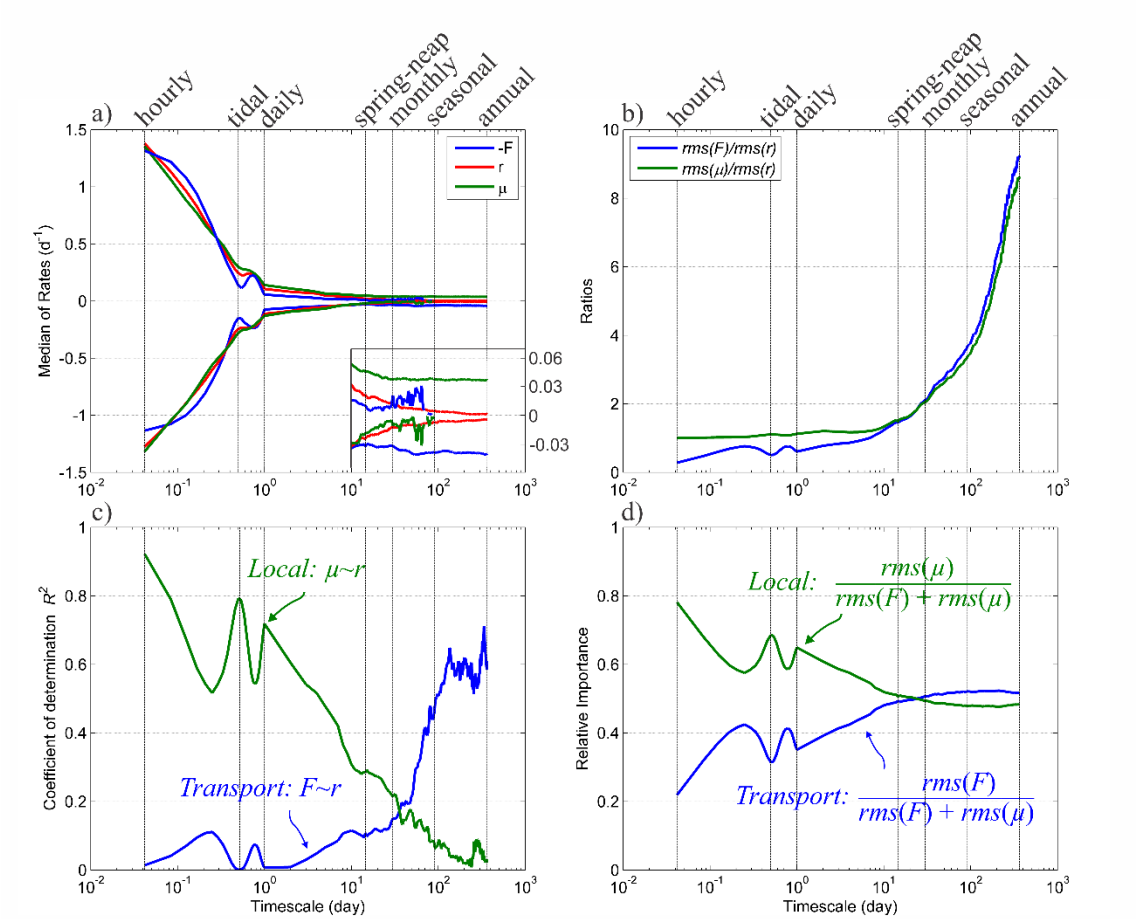

772

773 Fig. 6. a) Medians over different timescales for positive and negative rates, respectively.

774 Transport rate (–*F*, blue lines), relative growth rate *r* (red lines), and growth rate

775 μ (green lines); b) Ratios of root-mean-square of rates. Blue line denotes *rms*(*F*) to

776 *rms*(*r*), green line denotes *rms*(μ) to *rms*(*r*); c) coefficient of determination R^2 between *F*

777 and *r* (blue line) and between μ and *r* (green line); and d) estimates of the relative

778 importance of transport processes (blue line) and local processes (green line).

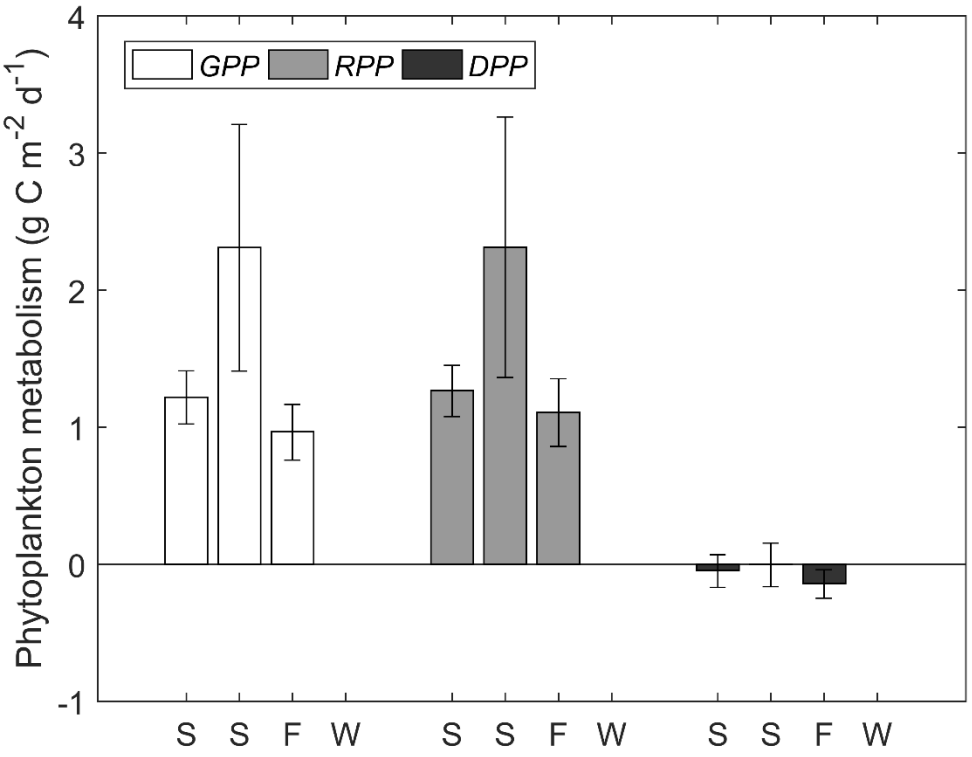

779

780 Fig. 7. Phytoplankton primary production in each season of 2008 at Station RC, by

781 assuming $FPP = F \cdot B$ (winter data are not available). Phytoplankton gross primary

782 productivity (*GPP*), phytoplankton total biological losses (*RPP*, including respiration,

783 grazing and settling), phytoplankton *DPP* (*GPP* - *RPP*), error bars represent the 95%

784 confidence intervals.